Brief Reports

Brief Reports are accounts of completed research which, while meeting the usual **Physical Review** *standards of scientific quality, do not warrant regular articles. A Brief Report may be no longer than four printed pages and must be accompanied by an abstract. The same publication schedule as for regular articles is followed, and page proofs are sent to authors.*

Thermodynamic model of the insulator-metal transition in nickel iodide

J. K. Freericks* and L. M. Falicov
Department of Physics, University of California, Berkeley, California 94720
and Materials Science Division, Lawrence Berkeley Laboratory, Berkeley, California 94720
(Received 16 May 1991)

A model calculation of the phase diagram for the isostructural insulator-metal phase transition of nickel iodide is presented. The system is modeled by the Falicov-Kimball Hamiltonian with the calculated band structure of NiI_2 and (Ising) spin-spin interactions, but neglects all hybridization effects between nickel $3d$ and iodine $5p$ bands. Many-body interactions and spin superexchange are both treated in mean-field theory. The results include second-order antiferromagnetic-paramagnetic insulator transitions, first-order insulator-metal transitions, and a (as yet unobserved and probably unobservable) classical critical point. The calculated phase diagram and transport properties agree well with the recent experimental results.

Nickel iodide (NiI_2) is a transition-metal halide that has been shown to exhibit an isostructural insulator-metal transition[1] (with a simultaneous collapse of antiferromagnetic order) upon the application of hydrostatic pressure. The experiments[1] utilize Mössbauer spectroscopy (of the isotope ^{129}I), conductivity, and x-ray-diffraction measurements within a diamond-anvil cell to observe this phase transition.

Nickel iodide crystallizes in the $CdCl_2$ ($R\bar{3}m$) structure, which consists of alternating hexagonal planes of nickel and iodine. The structure can be viewed as a face-centered-cubic lattice of I^- ions with every other close-packed (111) plane intercalated by a hexagonal plane of Ni^{2+} ions. The triple-layer neutral sandwich I^--Ni^{2+}-I^- compresses by approximately 2.5% along the c axis and forms a layered structure of weakly interacting sandwiches. The hexagonal lattice constants[2] are $a=3.922$ Å and $c=19.808$ Å. At low temperatures ($T<60$ K), nickel iodide undergoes a hexagonal-monoclinic distortion[2] that nonuniformly changes the planar lattice constants by an additional 0.25%.

Each Ni^{2+} ion contains a local ($S=1$) spin magnetic moment. At low temperatures these moments order[2] as an incommensurable helix of type 1 which is very nearly approximated by ferromagnetic planes of Ni^{2+} (with the spins oriented at an angle of 55° to the c axis) that are ordered antiferromagnetically along the c axis. The Néel temperature[1] is 75 K at ambient pressure and increases by over four orders of magnitude to 310 K at the metallization pressure of 19 GPa.

Band-structure calculations[3] (using the intersecting spheres approach) have been performed on the isostructural nickel dihalides $NiCl_2$ and $NiBr_2$. The crystal structure is taken to be the "ideal" structure in which the iodine-iodine interplanar spacing is not compressed by the intercalated Ni^{2+} plane. The calculated energy bands contain the following features: (i) the five nickel $3d$ bands break into groups of three bands and two bands with bandwidths of less than 0.5 eV; (ii) the Fermi level E_F lies within the upper group of two $3d$ bands; (iii) the uppermost three filled halogen p bands lie 2.0 eV (1.5 eV) below E_F and have a bandwidth of 2.0 eV (3.0 eV) for $NiCl_2$ ($NiBr_2$); (iv) two of the halogen p bands have, close to the top, cylindrical constant-energy surfaces with very little dispersion in the z direction.

The band-structure trend is to reduce the energy separation of the uppermost halogen p bands from the Fermi level and to increase the bandwidth of these p bands as the atomic size of the halogen increases (or equivalently as pressure is applied). In this manner, nickel iodide (at ambient pressure) can be predicted to have a Fermi level lying within a group of two nickel $3d$ bands and to have iodine $5p$ bands that lie approximately 1.0 eV below E_F with a bandwidth of approximately 4.0 eV. Band theory predicts that nickel iodide is a metal.

Many-body interactions[4] modify the one-electron picture for the electrons in the nickel $3d$ bands. The Ni^{2+} ion is described, to a first approximation, by a spin-triplet $3d^8$ configuration of atomic (localized) states. It is energetically unfavorable to form any atomic configuration with fluctuating charges (such as $3d^7 \leftrightarrow 3d^9$) so that the $3d$ electrons are frozen at the nickel sites and do not conduct.

The Falicov-Kimball model[5] was introduced 20 years ago to describe isostructural insulator-metal transitions. The model includes both uncorrelated conduction electrons (or holes) and strongly correlated localized electrons with the insulator-metal transition occurring when the localized electrons move into the conduction bands. The Hamiltonian is

$$H=\sum_{\nu,k,\sigma}\varepsilon_\nu(k)a^\dagger_{\nu k\sigma}a_{\nu k\sigma}+\varepsilon_d\sum_{i,\sigma}d^\dagger_{i\sigma}d_{i\sigma}-G\sum_{\nu,i,\sigma,\sigma'}c^\dagger_{\nu i\sigma}c_{\nu i\sigma}d^\dagger_{i\sigma'}d_{i\sigma'}+\sum_{i,j}J_{ij}(1-d^\dagger_{i\uparrow}d_{i\uparrow}-d^\dagger_{i\downarrow}d_{i\downarrow})\mathbf{S}_i\cdot\mathbf{S}_j(1-d^\dagger_{j\uparrow}d_{j\uparrow}-d^\dagger_{j\downarrow}d_{j\downarrow})\ , \tag{1}$$

where $a^\dagger_{\nu k\sigma}$ creates a Bloch hole in band ν with wave vector $\mathbf{k}$ and spin σ, $\varepsilon_\nu(k)$ is the (hole) band structure for the νth conduction band, $d^\dagger_{i\sigma}$ creates a d electron in a localized (atomic) orbital in the ith unit cell, ε_d is the energy to create a d electron, $c^\dagger_{\nu i\sigma}=\sum_{\mathbf{k}}\exp(-\mathbf{k}\cdot\mathbf{R}_i)a^\dagger_{\nu k\sigma}/\sqrt{N}$ creates a hole in a Wannier orbital localized about site $\mathbf{R}_i$, and G is the (excitonic) electron-hole interaction energy.[6] The last term in (1) is a Heisenberg spin-exchange interaction term for the localized spins $\mathbf{S}_i$ (that are present at the atomic sites i whenever[7] $\langle\sum_\sigma d^\dagger_{i\sigma}d_{i\sigma}\rangle=0$) and J_{ij} is the interaction energy between two localized spins at sites i and j. The Hilbert space is restricted to the subspace of states that include no doubly occupied localized electrons; i.e., $\langle\sum_\sigma d^\dagger_{i\sigma}d_{i\sigma}\rangle\le 1$. Charge neutrality requires that the number of conduction holes $\sum_{\nu,k,\sigma}a^\dagger_{\nu k\sigma}a_{\nu k\sigma}$ is equal to the number of localized electrons $\sum_{i,\sigma}d^\dagger_{i\sigma}d_{i\sigma}$. The model is mapped onto the case of NiI_2 as follows.

(i) The vacuum state corresponds to the d^8 configuration of Ni^{2+} ions with the interactions J_{ij} chosen so that the $(S=1)$ spins are oriented into ferromagnetic planes that are ordered antiferromagnetically.

(ii) The band structure $\varepsilon_\nu(k)$ corresponds to the three uppermost iodine $5p$ bands with a density of states $\rho(E)$ described by[8]

$$\rho(E)=\frac{\sqrt{E}}{3.72}+\begin{cases}(1/6.63)\cos^{-1}(1-10E) & 0\le E\le 0.2\\ (\pi/6.63) & 0.2\le E\le 6.5\ ,\end{cases} \tag{2}$$

for $0\le E\le 6.5$, where all energies are measured in eV, the density of states is normalized to include six electron states per unit cell, and the energy E is measured from the bottom of the hole conduction band (the minimal hole excitation energy is ε_h).

(iii) The minimal energy to create an electron-hole pair, $\Delta\equiv\varepsilon_h+\varepsilon_d$, is varied to mimic the effect of the hydrostatic pressure on the system.

This model only allows fluctuations between electronic configurations of the form $3d^8$ and $3d^9\underline{L}$ where $\underline{L}$ refers to a ligand hole. All hybridization effects between the nickel $3d$ and the iodine $5p$ bands have also been neglected.

Exact treatment of the many-body Hamiltonian (1) is complicated by the presence of both the Falicov-Kimball interaction term and the Heisenberg spin-exchange interaction term. The thermodynamics of a system governed by the Hamiltonian (1) is treated here in mean-field theory only, neglecting all fluctuations. The localized-electron number density (per unit cell) is defined to be ν and is constrained to equal the conduction-hole density

$$\nu=\int_{-\infty}^{\infty}f(E)\rho(E)dE\ , \tag{3}$$

where $f(E)$ is the occupation of the hole states with energy $E+\varepsilon_h$ at a temperature T. The quantum-mechanical $(S=1)$ spins are approximated by Ising $(S=1)$ spins with a Weiss molecular field. The sublattice magnetization (for the antiferromagnetic state) is defined to be $M\equiv g\mu_B S(1-\nu)x$, with μ_B the Bohr magneton, S the localized (Ising) spin, and $0\le x\le 1$ the dimensionless sublattice magnetization.

The trial free energy (per unit cell) becomes

$$\begin{aligned}F_1=&\int_{-\infty}^{\infty}\{(E+\varepsilon_h)f(E)+k_BTf(E)\ln f(E)+k_BT[1-f(E)]\ln[1-f(E)]\}\rho(E)dE\\&+\varepsilon_d\nu+k_BT[\nu\ln\nu+(1-\nu)\ln(1-\nu)]-k_BT\nu\ln 2-G\nu\int_{-\infty}^{\infty}f(E)\rho(E)dE\\&+\tfrac{1}{2}JS^2(1-\nu)^2x^2-k_BT(1-\nu)\ln\frac{\sinh[(S+\frac{1}{2})\beta JS(1-\nu)x]}{\sinh[\frac{1}{2}\beta JS(1-\nu)x]}+\lambda\left[\nu-\int_{-\infty}^{\infty}f(E)\rho(E)dE\right]\ ,\end{aligned} \tag{4}$$

which includes the free energy of the conduction holes, the free energy of the localized electrons, the Falicov-Kimball interaction energy, the free energy of the localized (Ising) spins, and the Lagrange multiplier term (with Lagrange multiplier λ) to ensure constraint (3). The magnetic interaction J is an effective magnetic-interaction term (that determines the Néel temperature) and the spin S is set to 1 for NiI_2. Performing the minimization of the trial free energy (4) with respect to $f(E)$, ν, x, and λ yield

$$x=\frac{\sinh[\beta J(1-\nu)x]}{\cosh[\beta J(1-\nu)x]+\frac{1}{2}}\ , \tag{5a}$$

$$f(E)=(1+[\nu/(1-\nu)]\{\cosh[\beta J(1-\nu)x]+\tfrac{1}{2}\}\times\exp[\beta(E+\Delta-2G\nu)])^{-1}\ , \tag{5b}$$

$$\nu=\int_{-\infty}^{\infty}f(E)\rho(E)dE\ , \tag{5c}$$

$$\begin{aligned}F_T=&G\nu^2+\tfrac{1}{2}J(1-\nu)^2x^2\\&+k_BT\ln((1-\nu)/\{2\cosh[\beta J(1-\nu)x]+1\})\\&+k_BT\int_{-\infty}^{\infty}\ln[1-f(E)]\rho(E)dE\ ,\end{aligned} \tag{5d}$$

where $\beta=1/k_BT$.

For general values of the temperature there are multi-

ple solutions to the transcendental equations (5a)–(5c) and the true solution corresponds to the absolute minimum of the free energy (5d). These solutions are characterized by their limiting behavior as $T \to 0$: antiferromagnetic insulators ($x \to 1, \nu \to 0$), paramagnetic insulators ($x = 0, \nu \to 0$), paramagnetic metals ($x = 0, \nu \to 1$), and nonphysical solutions ($x = 0, \nu \to \nu_{\text{nonphys}}$). The nonphysical solutions satisfy $0 < \nu_{\text{nonphys}} < 1$ and always have a corresponding free energy (5d) that is larger than all of the other solutions (for *all* values of the temperature).

There is always at least one paramagnetic ($x = 0$) solution to the transcendental equations (5a)–(5c). An antiferromagnetic insulator solution occurs whenever the temperature T satisfies

$$k_B T < \tfrac{2}{3} J[1 - \nu(T)] \tag{6}$$

and the Néel temperature T_N is defined by the largest temperature that satisfies (6). The antiferromagnetic solution always has a lower free energy ($F_T \to -\frac{1}{2}J$) than the paramagnetic insulator ($F_T \to 0$) in the limit of vanishing temperature ($T \to 0$). The paramagnetic metal solution and the nonphysical solution are present (at zero temperature) whenever the derivative of the internal energy with respect to the electron concentration is less than zero,

$$(\partial F_T(T \to 0)/\partial \nu)_{\nu=1, x=0} < 0 \tag{7a}$$

or

$$E_1 + \Delta - 2G < 0 , \tag{7b}$$

where $E_1 = 1.509$ eV is the Fermi level for one conduction hole per unit cell. The paramagnetic metal has the minimal free energy whenever the metallic free energy lies below $-\frac{1}{2}J$ as $T \to 0$, or

$$\tfrac{1}{2}J + \int_0^{E_1} E\rho(E)dE + \Delta - G < 0 , \tag{8}$$

where $\int_0^{E_1} E\rho(E)dE = 0.836\,85$ for the NiI_2 density of states (2).

As the temperature is increased from zero, the number of solutions to the transcendental equations (5a)–(5c) decreases:[5] as T is increased beyond the Néel temperature T_N the antiferromagnetic-insulator solution disappears undergoing a second-order transition to the paramagnetic-insulator phase at T_N; as T is increased beyond a temperature (denoted by $T_{3 \to 1}$) the nonphysical solution joins either the insulating solution or the metallic solution and both disappear leaving only one paramagnetic solution to the transcendental equations (5a)–(5c).

The parameters are chosen to be

$$G = 0.93 \text{ eV} ; \tag{9}$$

Δ is a function of pressure such that

$$\begin{aligned} &\Delta = 1.000 \text{ eV}, \quad P = 0 \text{ GPa} , \\ &\Delta = 0.075 \text{ eV}, \quad P = 19 \text{ GPa} ; \end{aligned} \tag{10}$$

and the effective magnetic interaction J is chosen to be a linear function of Δ,

$$J(\Delta) = (487 - 376\Delta)/11\,840 , \tag{11}$$

which yields a Néel temperature of 75 K at ambient pressure and 310 K at 19 GPa. The parameter G produces an insulator-metal transition at $\Delta \approx 0.08$ eV with a conduction-hole concentration that closely resembles the resistivity curves of Ref. 1 at 300 K.

The calculated phase diagram for NiI_2 is found in Fig. 1. The horizontal axis corresponds to the "pressure" axis and plots the parameter Δ in eV while the vertical axis corresponds to the temperature. The shaded region of Fig. 1 is the antiferromagnetic-insulator phase. The chain-dotted line is a second-order transition line from the antiferromagnetic insulator to the paramagnetic insulator and marks the Néel temperature as a function of "pressure." The white region above the chain-dotted line and to the left of the solid line is the paramagnetic-insulator phase. The solid line marks the first-order phase transition from an insulator to a paramagnetic metal. This insulator-metal transition line ends at a classical critical point at $T_c \approx 1400$ K and $\Delta_c \approx 0.03$ eV denoted by the open circle. Above the critical point there is no clear demarcation between a paramagnetic insulator and a metal. The dashed line in Fig. 1 indicates where the paramagnetic insulator-metal transition would occur in the absence of any magnetic order. Finally, the region below the dotted line is the region where there are three paramagnetic solutions to Eqs. (5a)–(5c) and the region above the dotted line has only one solution.

The insulator-metal transition line is very nearly vertical, but the slight curvature does allow the system to have a small range of Δ (a fixed pressure range) where there is a change from an antiferromagnetic insulator at low T to a metal at moderate T and then to a paramag-

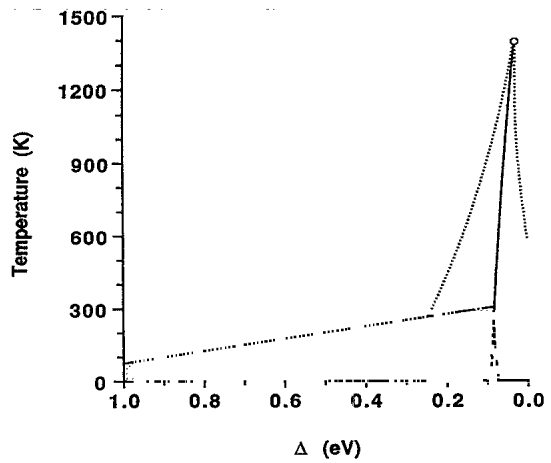

FIG. 1. Calculated phase diagram for nickel iodide (NiI_2). The horizontal axis approximately measures the pressure and the vertical axis measures the temperature. The shaded region corresponds to an antiferromagnetic insulator. The chain-dotted line is the second-order transition line from an antiferromagnetic insulator to a paramagnetic insulator. The solid line is the first-order insulator-metal transition line. The dotted line marks the temperature $T_{3 \to 1}$ where the number of paramagnetic solutions to the transcendental equations (5a)–(5c) changes from three to one. Note the appearance of a classical critical point at $T_c \approx 1400$ K and $\Delta_c \approx 0.03$ eV.

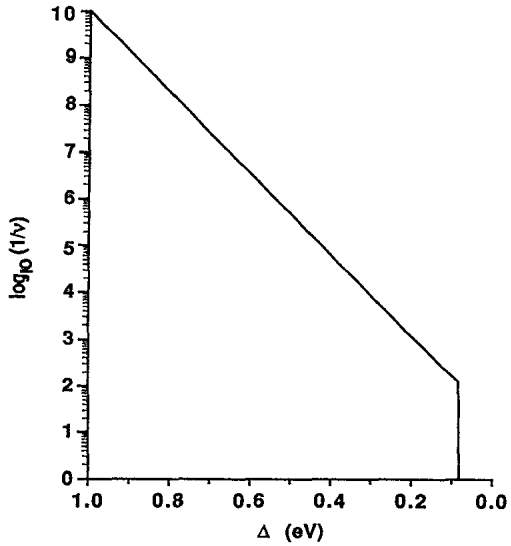

FIG. 2. Logarithm of the reciprocal conduction-hole concentration at a temperature of 300 K. Note that the reciprocal hole concentration has an exponential dependence on Δ and a jump of two orders of magnitude at the insulator-metal transition.

netic insulator at high T. The calculated critical point may not be physically accessible to the system. Nickel iodide decomposes at a temperature[2] of approximately 1000 K at ambient pressure. If this decomposition temperature increases fast enough with pressure, then NiI_2 may be another system with an observable classical critical point (similar[5] to the α-γ phase transition of cerium and the alloys of vanadium chromium oxide).

The logarithm of the reciprocal conduction-hole concentration $[\log_{10}(1/\nu)]$ is plotted in Fig. 2 as a function of Δ (pressure) at fixed temperature ($T=300$ K). This is the simplest approximation to the resistivity of NiI_2 as a function of pressure. The "resistivity" curve is almost exponential in Δ up to the point of the first-order metal-insulator transition, where it decreases discontinuously by two orders of magnitude. The slope of the logarithm of the "resistivity" and the magnitude of the jump agree quite well with the experimental results.[1]

At low temperature ($T\approx 4$ K) the sublattice magnetization jumps discontinuously from 1 to 0 at the first-order phase transition between the antiferromagnetic insulator and the metallic phase. The curvature that is present in the experimental data[1] is most likely due to the hybridization between nickel $3d$ and iodine $5p$ bands (that have been neglected here). The effect of hybridization on a simpler model[9] has shown this curvature.

In summary, a simple model of isostructural insulator-metal transitions has been applied to nickel iodine. The calculated phase diagram and resistivity curves agree quite well with the experimental data[1] and show the existence of a classical critical point. Several approximations have gone into this model calculation and they are summarized here.

(i) The effect of hybridization has been neglected. Inclusion of hybridization effects tends to "smooth out" the first-order phase transitions as illustrated in Ref. 9 for a simpler model.

(ii) The quantum-mechanical interactions of the ($S=1$) spins have been completely neglected. This is known to be a poor approximation for magnetic properties, but the change in the free energy arising from a more accurate treatment of the spins is much smaller than the electronic contributions and should not change the qualitative behavior described above.

(iii) Many-body corrections beyond mean-field theory for both the Falicov-Kimball interaction and the magnetic interaction should produce a much more accurate phase diagram.

(iv) A more accurate calculation of the transport properties that include resonance scattering of the conduction holes with the localized electronic states could produce a more realistic resistivity curve (rather than assuming that the resistivity was inversely proportional to the carrier concentration).

We acknowledge helpful discussions with A. Chen, A. Giesekus, and M. Pasternak. One of the authors (J.K.F.) acknowledges support of the Department of Education during the earlier stages of this work. This research was supported, at the Lawrence Berkeley Laboratory, by the Director, Office of Energy Research, Office of Basic Energy Sciences, Materials Science Division, U.S. Department of Energy, under Contract No. DE-AC03-76SF00098.

*Present address: Institute for Theoretical Physics, University of California, Santa Barbara, CA 93106-4030.

[1]M. P. Pasternak, R. D. Taylor, A. Chen, C. Meade, L. M. Falicov, A. Giesekus, R. Jeanloz, and P. Y. Yu, Phys. Rev. Lett. **65**, 790 (1990).

[2]S. R. Kuindersma, J. P. Sanchez, and C. Haas, Physica **111B**, 231 (1981).

[3]S. Antonici and L. Mihich, Phys. Rev. B **18**, 5768 (1979); **21**, 3383 (1980); J. Zaanen, doctoral thesis, Rijksuniversiteit te Groningen, Holland, 1986 (unpublished).

[4]N. F. Mott, *Metal-Insulator Transitions* (Taylor and Francis, London, 1974); J. Zaanen and G. A. Sawatzky, Prog. Theor. Phys. Suppl. **101**, 231 (1990).

[5]L. M. Falicov and J. C. Kimball, Phys. Rev. Lett. **22**, 997 (1969); R. Ramirez, L. M. Falicov, and J. C. Kimball, Phys. Rev. B **2**, 3383 (1970); R. Ramirez and L. M. Falicov, *ibid.* **3**, 2425 (1971); L. M. Falicov, C. E. T. Gonçalves da Silva, and B. Huberman, Solid State Commun. **10**, 445 (1972).

[6]The Falicov-Kimball interaction parameter G must be chosen small enough so that bound excitons do not form (for a further discussion, see Ref. 5).

[7]The localized electrons created by $d_{i\sigma}^{\dagger}$ are assumed not to have any spin-spin interactions.

[8]The density of states are determined by fitting the calculated band structure of Ref. 3 for $NiBr_2$. The fitted (hole) bands are

$$\varepsilon_1(k)=\varepsilon_h+0.1(1-\cos k_z/k_0)+0.15(k_x^2+k_y^2)/k_0^2\ ,$$

$$\varepsilon_2(k)=\varepsilon_h+0.1(1-\cos k_z/k_0)+0.4(k_x^2+k_y^2)/k_0^2\ ,$$

$$\varepsilon_3(k)=\varepsilon_h+0.375k_z^2/k_0^2+0.1(k_x^2+k_y^2)/k_0^2\ ,$$

where $k_0=3/c=0.152$ Å^{-1}, all energies are measured in eV, and ε_h is the minimal hole excitation energy.

[9]A. Giesekus and L. M. Falicov, Phys. Rev. B **44**, 10449 (1991).